JACS
JOURNAL OF THE AMERICAN CHEMICAL SOCIETY

ARTICLE

pubs.acs.org/JACS

Cyclopropylhydroxycarbene

David Ley, Dennis Gerbig, J. Philipp Wagner, Hans P. Reisenauer, and Peter R. Schreiner*

Justus-Liebig University, Heinrich-Buff-Ring 58, 35392 Giessen, Germany

Supporting Information

ABSTRACT: Cyclopropylhydroxycarbene was generated by high-vacuum flash pyrolysis of cyclopropylglyoxylic acid at 960 °C. The pyrolysis products were matrix-isolated in solid Ar at 11 K and characterized by means of IR spectroscopy. Upon photolysis, the carbene undergoes ring expansion, thereby paralleling the reactivity of other known cyclopropylcarbenes. The ring expansion product, cyclobut-1-en-1-ol, was characterized for the first time. Matrix-isolated cyclopropylhydroxycarbene undergoes [1,2]H-tunneling through a barrier of approximately 30 kcal·mol^{-1}, yielding cyclopropylcarboxaldehyde. The cyclopropyl moiety acts as a π-donor and increases the half-life by almost a factor of 10 compared to parent hydroxymethylene, resulting in a temperature-independent half-life of τ = 17.8 h at both 11 and 20 K. Hence, cyclopropylhydroxycarbene is the first hydroxycarbene that differs from other members of its family by a significantly prolonged half-life. As expected, the O-deuterated analogue does not show tunneling. Our findings are rationalized by accurate CCSD(T)/cc-pVnZ (n = D, T)//M06-2X/6-311++G(d,p) computations. The half-life of cyclopropylhydroxycarbene was verified by tunneling computations employing the Wentzel−Kramers−Brillouin formalism. By comparison with other experimentally known hydroxycarbenes, we determine the electronic donor capabilities of the carbenes' substituents to be a dominant factor governing their half-lives.

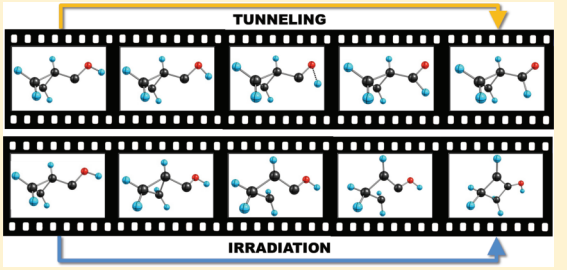

INTRODUCTION

In the chemistry of highly reactive alkylcarbenes, cyclopropylcarbenes are unique because the strained, three-membered ring is an excellent electron donor.[1,2] The electron deficiency of the carbene center leads to ring expansion reactions to the corresponding cyclobutenes, with the driving force arising from the addition of a double bond and from providing all carbon atoms with the desired electron octet. This ring expansion has been observed for cyclopropylmethylene[3−7] (**3a**) and its derivatives cyclopropylmethylcarbene[8,9] (**3b**) and cyclopropylchloro- and cyclopropylfluorocarbene (**3c,d**; see Scheme 1),[10−15] whose ring expansion reactions yield the cyclobutenes **4a**−**d**.[11,16−18] The driving force for this ring expansion facilitates the preparation of extremely strained cyclobutene derivatives.[19−21]

The carbene family has recently been extended by the class of hydroxycarbenes (**1**), for which a remarkable hydrogen tunneling mechanism in noble gas matrices was revealed, even at temperatures as low as 11 K.[22] The parent hydroxycarbene, hydroxymethylene (**1a**), decays through [1,2]H-tunneling with a measured half-life of τ = 2.0 h to give formaldehyde (**2a**). By analogy, phenylhydroxycarbene (**1b**)[23] and methylhydroxycarbene (**1c**)[24] give benzaldehyde (**2b**) and acetaldehyde (**1c**), respectively, with similar half-lives. However, in contrast to **1a**−**c**, the reactivities of dihydroxycarbene (**1d**) and methoxyhydroxycarbene (**1e**) are strikingly different.[25] Whereas all experimentally known hydroxycarbenes without heteroatoms other than that of the single hydroxy group undergo H-tunneling, hydroxycarbenes with a second heteroatom are persistent under cryogenic conditions (Scheme 1). This is most likely due to the increased overall positive mesomeric effect on the carbene center by two donor substituents. In the course of our ongoing investigations concerning the nature of H-tunneling and the factors that govern it, we sought to prepare a hydroxycarbene that constitutes an intermediate between the tunneling and nontunneling species known so far, that is, one with a considerably larger half-life than **1a**−**c**. Thus, we considered attaching to the hydroxycarbene center a π-donating group stronger than phenyl but weaker than oxygen. The unique electronic properties exhibited by the Walsh orbitals of the cyclopropyl moiety make

Scheme 1. Common Reactivity Patterns of Known Hydroxy- and Cyclopropylcarbenes

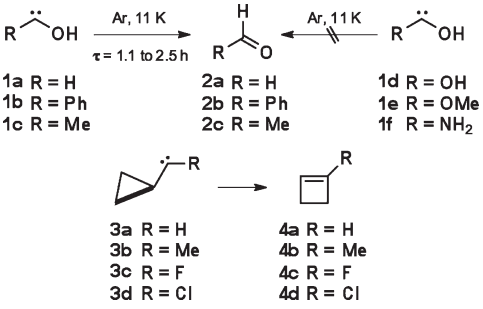

Received: May 29, 2011
Published: July 27, 2011

it a most suitable candidate for our efforts to increase the stability of **1** toward tunneling decay without entirely shutting down this pathway. Therefore, we sought to prepare and matrix-isolate cyclopropylhydroxycarbene (**3e**; Scheme 2). Regarding a possible ring expansion reaction of **3e** like in carbenes **3a**−**d**,[22,23] we were curious about the reactivity of **3e**.

RESULTS AND DISCUSSION

Preparation and Characterization of Cyclopropylhydroxycarbene 3e. Following our generic route for the preparation of hydroxycarbenes,[22−25] we obtained **3e** through thermal decarboxylation of cyclopropylglyoxylic acid (**6**), which is readily accessible through alkaline potassium permanganate oxidation of cyclopropylmethylketone (**5**).[26] Precursor **6** was evaporated from a small storage vial into the pyrolysis zone of the matrix apparatus (see Experimental Section for details); the pyrolyses were carried out at 600, 750, and 960 °C. In contrast to our previous work on other hydroxycarbenes, the matrix-isolated pyrolysis mixture from **6** contained only small amounts of the respective aldehyde, in this case cyclopropylcarboxaldehyde (**7**). The major product was identified as methyl vinyl ketone (**10**), which is most likely the last link in a chain of subsequent rearrangements involving ring expansion of **3e** to cyclobut-1-en-1-ol (**8**), electrocyclic ring opening, and eventual keto−enol tautomerism of the intermediate 2-hydroxybuta-1,3-diene (**9**) to yield **10** (Scheme 2). However, the pyrolysis mixture mainly consisted of **6**, **7**, **10**, and **3e** in an estimated ratio of approximately 10:5:8:1 (based on relative IR band intensities). Carbene **3e** was sufficiently present in the matrix and could unequivocally be identified by means of IR spectroscopy (Figure 1). No traces of cyclobutanone, the keto tautomer of **8**, could be found.

Scheme 2. Generation of 3e by Thermal Carbon Dioxide Extrusion from Precursor 6, as Well as Thermal and Photochemical Rearrangement Reactions

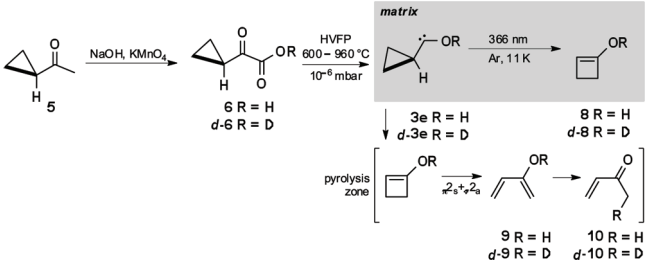

All characteristic IR absorptions (ν_{obs}) could be matched with the computed unscaled harmonic vibrational frequencies (ω_{theor}) of the energetically most favorable conformation **3et**$_{out}$ with the OH group pointing away from the cyclopropyl group and an s-*trans*-conformation of the HOCC moiety (Figure 1). The vibrational frequencies (Table 1a) were evaluated at the CCSD(T)/cc-pVTZ (frozen core, fc) (see Computational Details) level of theory.

The UV absorption maximum of **3et**$_{out}$, computed with time-dependent density functional theory (TD-DFT) at the B3LYP/6-311++G(d,p) level, was determined as λ_{max} = 373 nm ($^1A' \rightarrow {}^1A''$, open-shell). Accordingly, irradiation of the matrix at 366 nm resulted in complete disappearance of the respective signals. New signals appeared, though, which were in accordance with the computed spectrum of the primary ring expansion product **8**; a detailed discussion of **8**, which we characterize here for the first

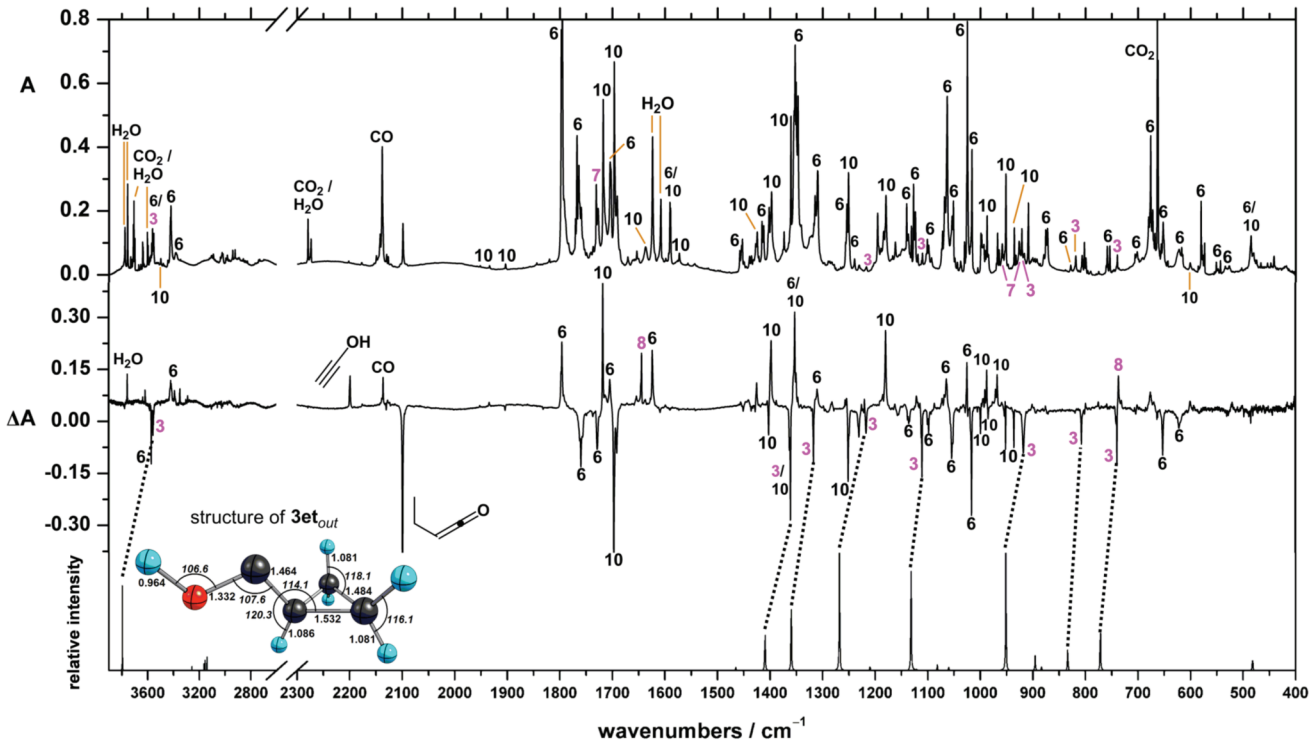

Figure 1. IR spectrum of pyrolysis mixture from **6** (top) and corresponding difference spectrum after 5 min of irradiation at 366 nm (middle); disappearing signals point downward and are matched with the unscaled computed spectrum of **3et**$_{out}$ (bottom) [CCSD(T)/cc-pVTZ]; new signals are due to the formation of **8**. (Inset) Structure of **3et**$_{out}$ optimized at CCSD(T)/cc-pVTZ. This pyrolysis was carried out at 960 °C, which is the highest possible temperature for our experimental setup. Lower temperatures resulted in a larger amount of remaining precursor **6** and thus a lower yield of **3e**.

dx.doi.org/10.1021/ja204507j |J. Am. Chem. Soc. 2011, 133, 13614–13621

Table 1. Unscaled Computed[a] Harmonic Vibrational Frequencies ω_{theor} of 3et$_{out}$ and *d*-3et$_{out}$

approx description	sym	ν_{obs} (cm^{-1})	I_{obs}	ω_{theor} (cm^{-1})	I_{theor} (km·mol^{-1})
(a) IR Bands of 3et$_{out}$					
OH str	a′	**3567**	w	3796	122
CCH def + COH def	a′	**1363**	s	1410	45
COH def + CCH def	a′	**1317**	s	1360	70
CO str	a′	**1217**	m	1268	130
COH def + CCH def	a′	**1112**	s	1132	114
		1110			
ring def	a′	**917**	m	952	125
ring def + OH oop def	a″	**807**	m	834	24
ring def + OH oop def	a″	**739**	s	772	51
(b) IR Bands of *d*-3e					
OD str	a′	**2637**	m	2764	71
CCH def	a′	**1352**	s	1396	92
CO str	a′	**1231**	s	1268	123
ring def	a′	**1158**	w	1202	34
ring def	a′			944	134
COD def + CH_2 oop def	a′	**824**	s	840	34

[a] CCSD(T)/cc-pVTZ.

Table 2. Unscaled Computed[a] Harmonic Vibrational Frequencies ω_{theor} of 8 and *d*-8

normal mode	sym	ν_{obs} (cm^{-1})	I_{obs}	ω_{theor} (cm^{-1})	I_{theor} (km·mol^{-1})
(a) IR Bands of **8**					
OH str	a′	**3618**	s	3823	51
C=C str	a′	**1644**	s	1693	180
COH def + CCH_2 str	a′	**1388**	w	1432	17
COH def + CH_2 wag	a′	**1220**	m	1246	62
COH def + CH_2 wag	a′	**1114**	w	1134	122
CCH oop def	a″	**737**	s	745	34
(b) IR Bands of *d*-**8**					
OD str	a′	**2670**	w	2782	34
C=C str	a′	**1646**	s	1691	171
COD def + CCH_2 str	a′			1370	82
COD def + ring def	a′			1009	68
CCH oop def	a′	**740, 737**	s	745	35

[a] CCSD(T)/cc-pVTZ.

time, is given below. In the initial spectrum of the pyrolysis mixture, a strong signal was found in the ketene region at 2099 cm^{-1}, which vanished upon irradiation at 366 nm. We assigned this band to but-1-en-1-one, which is likely to result thermally from **3e** in the pyrolysis tube and for which a TD-DFT computation at B3LYP/6-311++G(d,p) reveals a UV transition at 353 nm (^{1}A″ → ^{1}A′, open-shell). In addition, irradiation entailed a new signal at 2199 cm^{-1}, which matches the strongest band of matrix-isolated (Ar) hydroxyacetylene,[27] a fragmentation product of **3e** (see Supporting Information for further discussion). Other changes in signal intensities in the difference spectrum before and after irradiation of the matrix, depicted in Figure 1, originate from the interconversion of different rotamers of **10** and **6** (see next section on conformational analysis).

All matrix experiments with O-deuterated acid *d*-**6** were conducted accordingly, yielding the respective deuterated species *d*-**3e** (Table 1b) and *d*-**10** (through *d*-**7**, *d*-**8**, and *d*-**9**) as well as *d*-**8** (Table 2b) upon irradiation of *d*-**3e** at 366 nm. Bands of deuterated but-1-en-1-one and deuterated hydroxyacetylene were found at 2098 and 2198 cm^{-1}, respectively.

Conformational Analysis of Cyclopropylhydroxycarbene 3e. Two precursor rotamers are capable of extruding carbon dioxide, namely, **6t**$_{in}$ (methyne H and carbonyl O are *syn*) and **6t**$_{out}$ (methyne H and carbonyl O are *anti*), which lead to carbenes **3et**$_{out}$ and **3ec**$_{out}$ via **TS1** and **TS3**, respectively, with a very similar barrier for decarboxylation (Scheme 3). The two rotamers of **6** are separated by 1.4 kcal·mol^{-1} in favor of **6t**$_{out}$ and are connected by transition state **TS2** that lies +7.4 kcal·mol^{-1} above **6**$_{out}$ [CCSD(T)/cc-pVDZ//M06-2X/6-311++G(d,p)].

While pyrolysis at 960 °C allows the equilibration of both carbene conformers, **3et**$_{out}$ is thermodynamically favored; conformer **3ec**$_{out}$ could not be detected in the matrix. Whereas the rotation around the central carbon−carbon bond is almost barrierless for related structure **1c**, it is more hindered in **3e** due to the overlap between the empty p-orbital on the carbene center and the occupied Walsh-type orbital of the cyclopropyl moiety (Figure 2).

The degree of Walsh orbital interaction is evident in the conformational analysis of the rotation around the exocyclic carbon−carbon bond (rotation of OH) in **3e**, devised from a relaxed scan of the potential energy surface at the M06-2X/6-311++G(d,p) level (Scheme 4): By forcing the COH moiety into the molecular plane, the central p-orbital becomes perpendicular to the Walsh-type orbital, resulting in zero overlap and thus leading to an energetically unfavorable arrangement. This conformation is responsible for the sizable rotational barrier of 10.1 kcal·mol^{-1}. An even higher barrier was found earlier for parent **3a**.[6] During rotation of the hydroxy group in **3e**, two minima are passed, namely, **3et**$_{out}$ and **3ec**$_{out}$, which are only 1.8 kcal·mol^{-1} apart in favor of the **3et**$_{out}$ conformer. A similar scan of **1b** and **1c** reveals in both cases a lower barrier of C−C rotation compared to **3e** (0.9 and 6.9 kcal·mol^{-1}, respectively), which shows that the stabilizing effect of the interaction of the empty p-orbital with a Walsh-type orbital of the cyclopropyl group is indeed much larger than in **1b** or **1c**.

For structural and reactivity comparisons, both parent systems of **3e** have to be considered, namely, cyclopropylcarbenes and hydroxycarbenes (Scheme 5, bottom). While the exocyclic carbon−carbon bond in **3et**$_{out}$ is long compared to other members of the cyclopropylcarbene family, it is short in comparison to the other known hydroxycarbenes (**1b**,**c**), demonstrating the strong interaction of the occupied Walsh-type orbital with the carbene's empty p-orbital. The empty p-orbital of the carbene center is partly saturated by substituents with strong electron-donor capabilities, enforcing the carbene's singlet character [ΔE_{ST} = 35.4 kcal·mol^{-1} at CCSD(T)/cc-pVTZ//M06-2X/6-311++G(d,p)]. Hence, the electron-donor strength of a substituent can be associated with the magnitude of the carbene's singlet−triplet gap ΔE_{ST}. This value can be used as a comparative measure for a substituent's electron-donor strength toward the empty p-orbital of the carbene center. Scheme 5 correlates the substituent's electron-donor strength with the length of the

Scheme 3. Two Conformers of Precursor 6 and Their Reactions Leading to 3e[a]

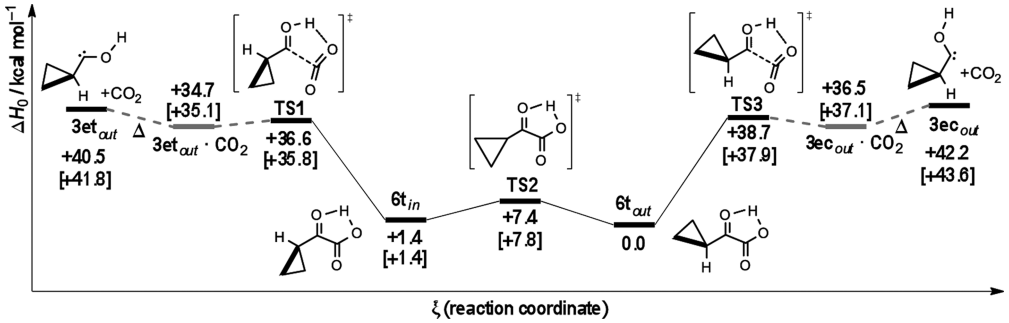

[a] After decarboxylation, a weakly bound complex of the carbene and CO_2 ($\mathbf{3et}_{out}\cdot CO_2$ or $\mathbf{3ec}_{out}\cdot CO_2$) can computationally be located but is not persistent at the pyrolysis temperatures and immediately dissociates into the carbene and carbon dioxide. Regular type = CCSD(T)/cc-pVDZ//M06-2X/6-311++G(d,p); in brackets = M06-2X/6-311++G(d,p).

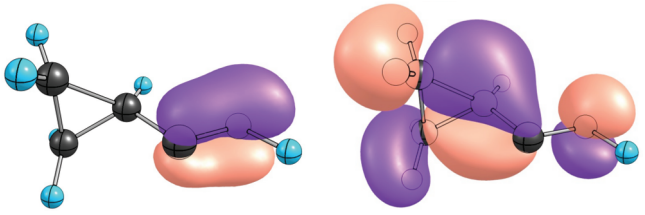

Figure 2. (Left) HOMO−5 orbital arising from electron donation from the oxygen p-orbital to the empty p-orbital of the carbene center. (Right) Interaction of the Walsh orbital with the empty p-orbital of the central carbon (middle lobe) in the HOMO−1 natural bond orbital [M06-2X/6-311++G(d,p)]. The displayed interactions stabilize the carbene center through n → p overlap, enhancing the singlet character of the carbene.

distal carbon−carbon bond (top) and the adjacent carbon−carbon bond (bottom): For members of the cyclopropylcarbene family, stronger electron-donating substituents increase this bond length and thus weaken both the adjacent as well as the distal carbon−carbon bond.[28] In hydroxycarbenes, stronger electron-donating substituents decrease the carbon−carbon bond length adjacent to the carbene center and thereby strengthen the bond. Being a member of both families, **3e** is located at the intersection of both lines. Only **1c** (in parentheses) slightly deviates from the observed trends.

Identification and Characterization of Cyclobut-1-en-1-ol 8. By comparison with the computed frequencies, the main photolysis product of **3e** could be identified as the cyclobutenol **8**, with the OH proton pointing toward the double bond (Figure 3). The C_s symmetrical molecule features a rhomboidal shape as the cyclobutene scaffold is strongly distorted by the OH group: The endocyclic double bond is the shortest bond in the ring (1.348 Å) facing the longest endocyclic single bond (1.573 Å), but the two other opposing single bonds also have significantly different lengths (1.506 versus 1.572 Å). The length of the corresponding double bond in vinyl alcohol is 1.337 Å compared to 1.348 Å in **8**. It should be noted that the cyclobutene moiety in **8** exhibits an even higher ring strain than the cyclopropyl moiety in **3e**.[29] The amount of strain energy strongly favors the ring-opening reaction in the hot pyrolysis zone so that intermediate **8** cannot be trapped directly in the pyrolysis mixture, but it can be generated from **3e** through irradiation. Yet **8** is stable toward

Scheme 4. Energy Profiles for Rotation around Central Carbon−Carbon Bonds in 1b, 1c, and 3e[a]

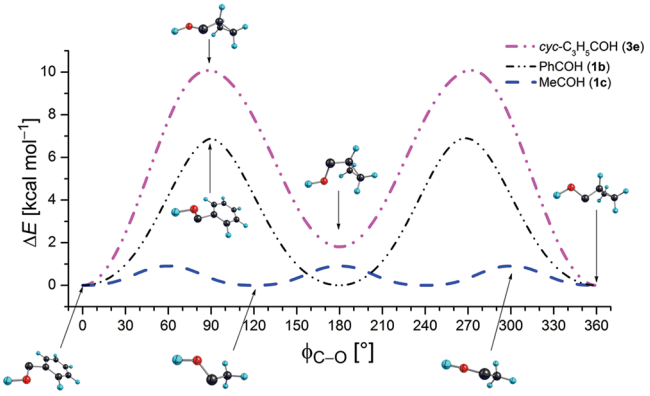

[a] M06-2X/6-311++G(d,p), not corrected for zero-point vibrational energies.

irradiation with wavelengths of 290 nm ≤ λ ≤ 800 nm. In accordance, the computed UV spectrum [B3LYP/6-311++G(d,p)] of **8** shows no absorptions above 300 nm. The observed vibrational frequencies (ν_{obs}) of **8** are listed in Table 2 and are matched with the computed harmonics (ω_{theor}).

Expansion and Rearrangement Reactions in the Pyrolysis Zone. All energies given in this paragraph have been computed at the CCSD(T)/cc-pVTZ//M06-2X/6-311++G(d,p) + ZPVE level unless stated otherwise. As found for other cyclopropylcarbenes, the ring expansion of **3e** via **TS4** is favored over all other reactions during the passage of the pyrolysis zone, and the interaction of electron-rich cyclopropyl orbitals with empty p-orbital at the carbene center generally promotes the C-shift over the H-shift in cyclopropylcarbenes.[11,16] The expansion takes place in the pyrolysis zone as the temperature is high enough to overcome the barrier of approximately +21 kcal·mol^{-1}. The energetically less favorable conformer $\mathbf{3ec}_{out}$ could in principle also undergo ring expansion, yet with a huge barrier of almost +52 kcal·mol^{-1}. The reaction sequence starting from ring expansion product **8** to **10** proceeds exothermically with about −22 kcal·mol^{-1}, and the energy arising from the transformation of **3e** to **8** (approximately −36 kcal·mol^{-1}) likely facilitates the electrocyclic ring opening of **8** to **9** via **TS5**, which is mainly

driven by the decrease in ring strain.[29] The subsequent [1,3]H-shift in **9** finally gives **10** via **TS6** (Scheme 6). The yields of these reactions cannot be estimated reliably, owing to the unknown absorption coefficients of the products. No traces of cyclopropylidenemethanol (**12**), the product of a thermal [1,2]H-shift via **TS7** from the α-carbon of the cyclopropyl moiety to the carbene center, were found, due to the high reaction barrier of approximately +36 kcal·mol^{-1}. A C−H insertion in **3e** via **TS8** would lead to highly strained and thus energetically unfavorable bicyclo-[1.1.0]butan-2-ol (**13**) and is furthermore hindered by a barrier of approximately +35 kcal·mol^{-1}. In accordance with these computational results, **13** was not observed experimentally.

Scheme 5. Correlation of (top) Distal Carbon−Carbon Bond Lengths in Some Cyclopropylcarbenes and (bottom) Adjacent Carbon−Carbon Bond Lengths in Hydroxy- and Cyclopropylcarbenes with ΔE_{ST}[a]

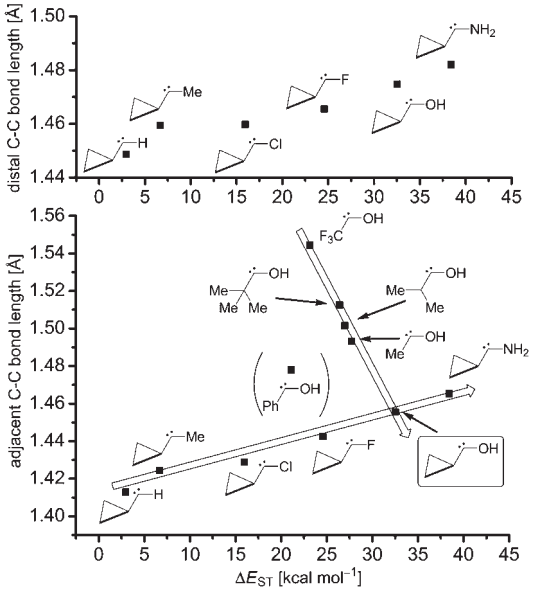

[a] ΔE_{ST} = singlet−triplet gap of carbenes. All structures were computed at the M06-2X/6-311++G(d,p) level.

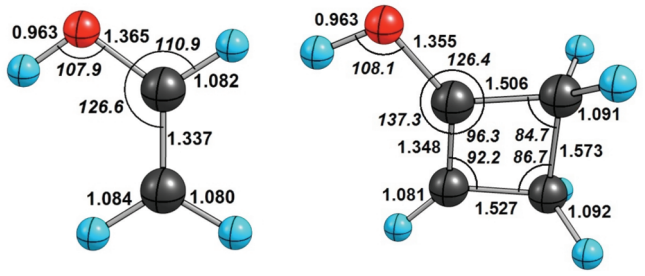

Figure 3. Structures of vinyl alcohol (left) and cyclobut-1-en-1-ol **8** (right), optimized at the CCSD(T)/cc-pVTZ level of theory.

[1,2]H-Tunneling in Cyclopropylhydroxycarbene 3e. The structure of **3e** sits in a deep energy minimum on the potential energy hypersurface, and the surrounding enthalpic barriers are too high to be overcome at cryogenic temperatures. In this regard, **3e** should be persistent in the matrix. However, even in the dark, the signals of matrix-isolated **3e** slowly vanish over the course of several hours to yield cyclopropylcarboxaldehyde (**7**) by transfer of the hydroxy H to the central carbon atom (Scheme 7). The increase of **7** could unequivocally be detected by means of IR spectroscopy (see Supporting Information). As for other hydroxycarbenes, the temperature-independent decay is likely to be due to a [1,2]H-tunneling mechanism and follows first-order kinetics. The half-life of **3e** was determined experimentally to be τ = 17.8 h at both 11 and 20 K, which is the longest half-life known to date for all hydroxycarbenes undergoing [1,2]H-tunneling.[22,23] The temperature independence of the first-order decay constant for the generation of **7** from **3e** and the unreactivity of *d*-**3e** are in accordance with a quantum mechanical tunneling mechanism. Employing the same theoretical Wentzel−Kramers−Brillouin (WKB) approach[30] as for **1a**−**c** (see Computational Details), the half-life of **3e** was computed to be τ = 16.6 h, in excellent agreement with experiment. In contrast, the O-deuterated species (*d*-**3e**) persistent under the same conditions as the tunneling mechanism is suppressed by the higher mass of deuterium, resulting in a computed half-life of approximately 10^5 years.

The tunneling mechanism favors the reaction of **3e** toward more stable product **7**, which is, however, kinetically disfavored. The H-tunneling in **3e** effectively reverses the expected reactivity (i.e., no reaction at cryogenic temperatures) under the conditions applied. In order to induce ring expansion of matrix-isolated **3e** to yield **8**, irradiation is necessary (see above). Since even at cryogenic temperatures the kinetically disfavored pathway is populated, the classical reactivity of the system is inverted by

Scheme 6. Potential Energy Surface of 3e Featuring H- and C-Migrations[a]

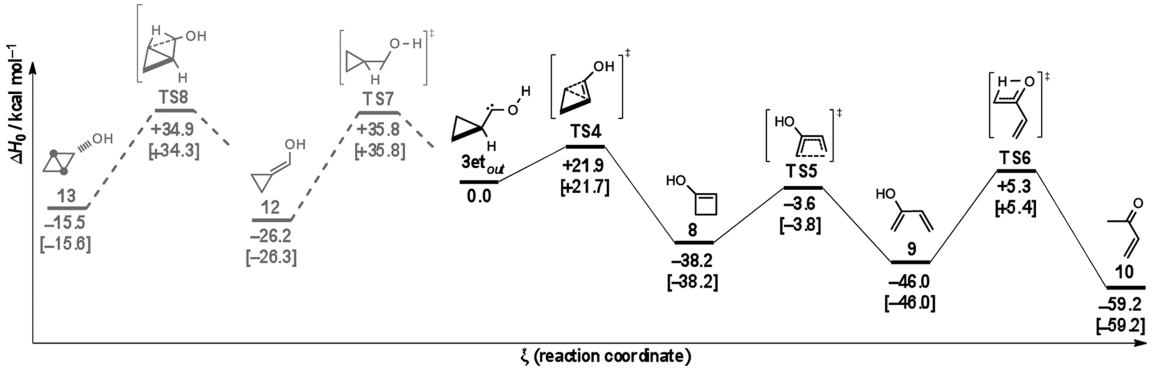

[a] Products of the reactions in gray are not observed experimentally. Computations are based on the most stable conformers of all species. Boldface type = CCSD(T)/cc-pVTZ//M06-2X/6-311++G(d,p) + ZPVE; lightface type = M06-2X/6-311++G(d,p) + ZPVE.

Scheme 7. Details of the Potential Energy Hypersurface of 3e Featuring both Kinetic and Tunneling Reaction Paths[a]

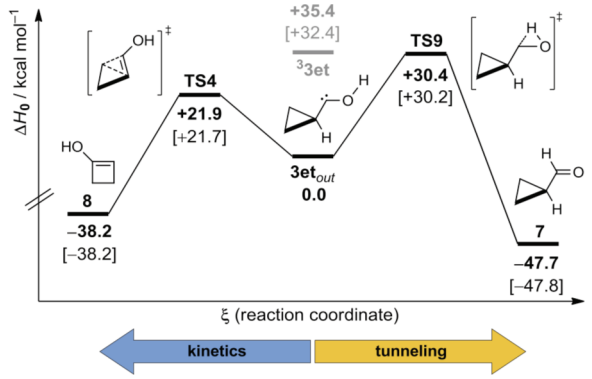

[a] Boldface type = CCSD(T)/cc-pVTZ//M06-2X/6-311++G(d,p) + ZPVE; lightfacce type = M06-2X/6-311++G(d,p) + ZPVE.

Scheme 8. Correlation of Hydroxycarbene Half-Life τ and Relative Electron-Donating Capability of Substituent[a]

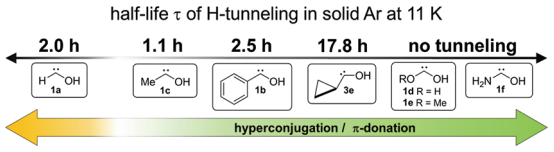

[a] Substituent = H, Me, Ph, *cyc*-C_3H_5, HO, MeO, or H_2N.

the tunneling mechanism, as observed for the related **1b**.[24] That is, *tunneling control* directs the reaction path away expected from classic kinetic control.

Correlation of Substituent's Electron-Donor Capabilities with Hydroxycarbene Half-Lives. The half-life of τ = 17.8 h suggests that the electronic effect of the cyclopropyl moiety on the carbene center is just enough to keep the H-tunneling decay at an observable rate, whereas heteroatomic π-donors, that is, −OH or $-OCH_3$, completely suppress [1,2]H-tunneling in the hydroxycarbenes **1d** and **1e**. The large singlet−triplet energy gap ΔE_{ST} also reflects the stabilizing effect exhibited by the cyclopropyl moiety (Schemes 5 and 7): The first triplet state of **3e**, for which the energetically most favorable conformation is ^{3}**3et**$_{in}$, with the OH group pointing toward the cyclopropyl group and an s-*trans*-conformation of the HOCC moiety, lies about +35 kcal·mol^{-1} higher in energy than the singlet state. The increase in half-life with an additional electron-donating substituent attached to the carbene's central carbon atom is also evident for the other members of the hydroxycarbene family, namely **1a**−**c** and aminohydroxycarbene **1f**. By qualitatively correlating a hydroxycarbene's half-life and the relative electron donor strength of its substituent, the currently known hydroxycarbenes can be arranged in a sequence of ascending stability (Scheme 8).

In **1c**, the methyl group stabilizes the carbene through hyperconjugation. In **1b** and **3e**, the substituents' connecting carbons are (effectively) sp^2-hybridized and exhibit a slight −I effect, which is overcompensated by the +M effect of the phenyl and cyclopropyl moieties, respectively. This influence is stronger in **3e**, resulting in an increased half-life. For stronger π-donors like oxygen and even more so nitrogen, [1,2]H-tunneling cannot be observed experimentally. Although the heteroatom +M effect

Scheme 9. Correlation of Hydroxycarbene Half-Life τ and Electron-Donating Capability of the Substituent[a] with an Isodesmic Relationship

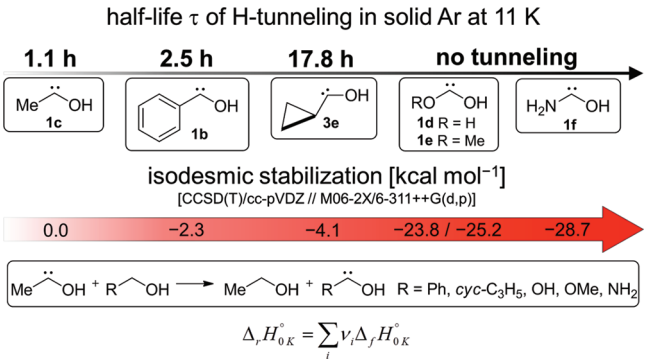

[a] Substituent = H, Me, Ph, *cyc*-C_3H_5, OH, OMe, or NH_2.

is accompanied by polarization of the σ-bond due to a noticeable difference in electronegativity, the interaction of the hydroxy, methoxy, and amino groups with the empty p-orbital overcompensates bond polarization and renders **1d**−**f** stable toward H-tunneling. Parent **1a** is the only carbene that has no carbon attached to its carbene center and is therefore expected to deviate from the above-mentioned relationship.

Isodesmic Evaluation of Hydroxycarbene Relative Stabilities with Respect to Tunneling. In order to further investigate the relationship between half-life and substituent electron-donating capability, we devised an isodesmic equation that describes these relative stabilities (Scheme 9):

The reaction enthalpies $\Delta_r H_0$ at 0 K of these hypothetical reactions are computed at the CCSD(T)/cc-pVDZ//M06-2X/6-311++G(d,p) and CCSD(T)/cc-pVDZ//B3LYP/6-311++G(d,p) levels (see Supporting Information for the latter) for the most stable conformers of all species involved; $\Delta_r H^\circ_{0K}$ corresponds to the gain in energy by exchanging carbene **1c** for **1b**, **1d**−**f**, and **3e**. The relative isodesmic stabilization energies become increasingly negative in the sequence of increasing half-life (Scheme 9). Although evaluation of the isodesmic equation only assesses the carbenes' relative thermodynamic stabilities, the latter depend on the electron-donor strength of the substituents. Thus, the carbenes' half-lives can indirectly be correlated with electron-donating capability of the substituents: More enthalpically stable hydroxycarbenes, which are indeed those with stronger electron-donating substituents, are those that have longer half-lives under cryogenic conditions.

CONCLUSION AND OUTLOOK

The ambivalent reactivity of hitherto unknown cyclopropylhydroxycarbene **3e** renders it both a typical cyclopropylcarbene and a distinctive hydroxycarbene that undergoes H-tunneling. The ring expansion of **3e** is similar to the reactions of carbenes **3a**−**d** and yields hitherto unknown cyclobutenol **8**, which undergoes further thermal reactions. In solid Ar at cryogenic temperatures, the characteristic [1,2]H-migration in **3e** occurs by quantum mechanical tunneling, as observed for **1a**−**c**. The lifetime of **3e** under inert matrix conditions is increased by the interaction of the carbene's empty p-orbital and the Walsh-type orbitals of the cyclopropyl donor, demonstrating the significance of π-effects on the H-tunneling phenomenon at work in hydroxycarbenes.

Fine-tuning of the substituent's electronic nature will be the key step to fully understand tunneling control at work in hydroxycarbenes and related systems.

COMPUTATIONAL DETAILS

The potential energy surface (PES) surrounding **3e** was established by employing density functional theory (DFT) at the M06-2X/6-311++G(d,p)[31,32] and B3LYP/6-311++G(d,p)[33−35] levels. The computed structures were then augmented with high-level coupled-cluster single and double excitation (with triple excitations) [CCSD(T)][36−39] energies (using the frozen-core approximation throughout), utilizing the ORCA[40,41] program package with the Dunning-type correlation-consistent basis sets cc-pVDZ and cc-pVTZ.[42] Geometry optimizations and frequency computations at the coupled-cluster level were carried out with the CFOUR program package, which features analytic first and second derivatives.[43] All computed harmonic vibrational frequencies presented in this work are unscaled. In general, the cc-pVTZ basis was used whenever computationally feasible. Otherwise, the less demanding cc-pVDZ basis set was employed. For the WKB evaluation of the half-life τ, the intrinsic reaction path[44] (IRP, starting from **TS9**) and the zero-point vibrational energy corrections (ZPVE) of the projected frequencies along the path were computed at the M06-2X/6-311++G(d,p) level using the Hessian-based predictor corrector algorithm[45] as implemented in Gaussian09.[46] Among many tested DFT functionals, the M06-2X functional was found to give half-lives closest to the experimental ones in theoretical tunneling examinations of the other known hydroxycarbenes.[22,23] A triple-ζ basis set is generally necessary to ensure an accurate IRP generation, at which, averaged over the half-lives of all currently known hydroxycarbenes, the 6-311++G(d,p) Pople basis has been found to be slightly superior to the cc-pVTZ Dunning basis. The tunneling probabilities were evaluated by computing one-dimensional barrier action integrals along the IRP and invoking the WKB relation. The attempt energy of the tunneling particle was set equal to the zero-point energy of the frequency corresponding to the reaction coordinate ξ. Algebraic equations were solved with the Mathematica program package.[47]

Despite the good results for **3e**, though, the one-dimensional WKB treatment of the [1,2]H-tunneling reaction has a serious caveat: Whereas the DFT-computed half-life of **3e** is in good agreement with the experimental results, a tunneling computation including CCSD(T)/cc-pVTZ energies on all points of the DFT-generated IRP greatly underestimates the lifetime of **3e**, mainly due to a significantly reduced reaction barrier at the coupled cluster level. Yet CCSD(T) results of other hydroxycarbenes are in very good agreement with their experimental half-lives even on DFT-generated paths. We are currently examining this apparent dichotomy, which is most probably due to the relatively small cc-pVTZ basis set used for the evaluation of single point energies with respect to this particular computational problem.

EXPERIMENTAL SECTION

Matrix Apparatus Design. For the matrix isolation studies, we used an APD Cryogenics HC-2 cryostat with a closed-cycle refrigerator system, equipped with an inner CsI window for IR measurements. Spectra were recorded with a Bruker IFS 55 FT-IR spectrometer with a spectral range of 4500−300 cm^{-1} and a resolution of 0.7 cm^{-1}. For the combination of high-vacuum flash pyrolysis with matrix isolation, we employed a small, home-built, water-cooled oven, which was directly connected to the vacuum shroud of the cryostat. The pyrolysis zone consisted of an empty quartz tube with an inner diameter of 8 mm, which was resistively heated over a length of 50 mm by a coaxial wire. The temperature was monitored with a NiCr−Ni thermocouple. Cyclopropylglyoxylic acid (**6**) was evaporated at −20 °C from a storage bulb into the quartz pyrolysis tube. At a distance of approximately 50 mm, all pyrolysis products were co-condensed with a large excess of argon (typically 60−120 mbar from a 2000 mL storage bulb) on the surface of the matrix window at 11 K (20 K). Several experiments with pyrolysis temperatures ranging from 600 to 960 °C were performed in order to determine the optimal pyrolysis conditions. A high-pressure mercury lamp (HBO 200, Osram) with a monochromator (Bausch & Lomb) was used for irradiation.

Preparation of Cyclopropylglyoxylic Acid (6).[26] To a mechanically stirred solution of 5.05 g (60 mmol) of cyclopropyl methyl ketone (**5**) in 30 mL of aqueous NaOH at 0 °C in a 250 mL round-bottom flask was added dropwise, over 3 h, a solution of 18.96 g (120 mmol) of $KMnO_4$ in 480 mL of H_2O. The reaction mixture was stirred overnight and allowed to warm up to 25 °C. After MnO_2 was filtered off, the volume of the clear, colorless filtrate was reduced in vacuo to approximately 100 mL. Then 7.05 g of aqueous HCl (37%) was added, and the reaction mixture was extracted three times with approximately 20 mL of CH_2Cl_2 each time. The combined organic layers were dried over Na_2SO_4 and the solvent was removed. Due to partial decarboxylation and reoxidation of the generated aldehyde, the crude mixture contained small amounts of cyclopropylcarboxylic acid and was hence fractionally distilled in vacuo. The O-deuterated precursor (*d*-**6**) was generated by repeated dissolution of **6** in D_2O, followed by evaporation of the solvent. Matrix experiments with *d*-**6** were conducted accordingly.

Colorless liquid, 1.8 g (16 mmol, 27% yield). ^1H NMR (400 MHz, $CDCl_3$) δ = 1.23−1.31 (4H, m), 2.84−2.90 (1H, m), 10.27 (1H, s); ^{13}C NMR (100 MHz, $CDCl_3$) δ = 15.51 (CH_2), 17.08 (CH), 160.77 (COCOOH), 195.35 (COCOOH); UV/vis (EtOH) λ_{max} (ε) = 330 nm (29 $mol^{-1}\cdot dm^3\cdot cm^{-1}$).

ASSOCIATED CONTENT

Supporting Information. Twenty-four figures, nine schemes, and nine tables showing full-matrix IR spectra of pyrolyses of **6** and *d*-**6** and reference spectra of **7** and **10**, both before and after irradiation at 366 nm; discussion of fragmentation products hydroxyacetylene and but-1-en-one; alternative version of Figure 1 featuring B3LYP/6-311++G(d,p) frequencies with anharmonic corrections; B3LYP/6-311++G(d,p) structures and corresponding CCSD(T) energies; and full references for electronic structure codes. This material is available free of charge via the Internet at http://pubs.acs.org.

AUTHOR INFORMATION

Corresponding Author
prs@org.chemie.uni-giessen.de

ACKNOWLEDGMENT

We gratefully acknowledge funding by the Deutsche Forschungsgemeinschaft (Grant Schr 597/13-1). D.L. thanks the Fonds der Chemischen Industrie for a scholarship, and D.G. thanks the Justus-Liebig University for a Graduiertenstipendium. We thank Wesley D. Allen and Attila G. Császár for helpful discussions.

REFERENCES

(1) de Meijere, A. *Angew. Chem., Int. Ed.* **1979**, *18*, 809–826.
(2) de Meijere, A.; Kozhushkov, S. I. *Chem. Rev.* **2000**, *100*, 93–142.
(3) Hoffmann, R.; Zeiss, G. D.; Van Dine, G. W. *J. Am. Chem. Soc.* **1968**, *90*, 1485–1499.
(4) Schoeller, W. W. *J. Org. Chem.* **1980**, *45*, 2161–2165.

(5) Wang, B.; Deng, C. *Tetrahedron* **1988**, *44*, 7355–7362.
(6) Shevlin, P. B.; McKee, M. L. *J. Am. Chem. Soc.* **1989**, *111*, 519–524.
(7) Chou, J. H.; McKee, M. L.; De Felippis, J.; Squillacote, M.; Shevlin, P. B. *J. Org. Chem.* **1990**, *55*, 3291–3295.
(8) Modarelli, D. A.; Platz, M. S.; Sheridan, R. S.; Ammann, J. R. *J. Am. Chem. Soc.* **1993**, *115*, 10440–10441.
(9) Thamattoor, D. M.; Jones, M.; Pan, W.; Shevlin, P. B. *Tetrahedron Lett.* **1996**, *37*, 8333–8336.
(10) Moss, R. A.; Fantina, M. E. *J. Am. Chem. Soc.* **1978**, *100*, 6788–6790.
(11) Liu, M. T. H.; Bonneau, R. *J. Phys. Chem.* **1989**, *93*, 7298–7300.
(12) Ho, G. J.; Krogh-Jespersen, K.; Moss, R. A.; Shen, S.; Sheridan, R. S.; Subramanian, R. *J. Am. Chem. Soc.* **1989**, *111*, 6875–6877.
(13) Bonneau, R.; Liu, M. T. H.; Rayez, M. T. *J. Am. Chem. Soc.* **1989**, *111*, 5973–5974.
(14) Moss, R. A.; Ho, G. J.; Shen, S.; Krogh-Jespersen, K. *J. Am. Chem. Soc.* **1990**, *112*, 1638–1640.
(15) Moss, R. A.; Liu, W.; Krogh-Jespersen, K. *J. Phys. Chem.* **1993**, *97*, 13413–13418.
(16) Moss, R. A.; Ho, G. J.; Liu, W. *J. Am. Chem. Soc.* **1992**, *114*, 959–963.
(17) Moss, R. A.; Jang, E. G.; Fan, H.; Wlostowski, M.; Krogh-Jespersen, K. *J. Phys. Org. Chem.* **1992**, *5*, 104–107.
(18) Ammann, J. R.; Subramanian, R.; Sheridan, R. S. *J. Am. Chem. Soc.* **1992**, *114*, 7592–7594.
(19) Wiberg, K. B.; Burgmaier, G. J.; Warner, P. *J. Am. Chem. Soc.* **1971**, *93*, 246–247.
(20) de Meijere, A.; Wenck, H.; Kopf, J. *Tetrahedron* **1988**, *44*, 2427–2438.
(21) de Meijere, A.; von Seebach, M.; Zöllner, S.; Kozhushkov, S. I.; Belov, V. N.; Boese, R.; Haumann, T.; Benet-Buchholz, J.; Yufit, D. S.; Howard, J. A. K. *Chem.—Eur. J.* **2001**, *7*, 4021–4034.
(22) Schreiner, P. R.; Reisenauer, H. P.; Pickard, F. C., IV; Simmonett, A. C.; Allen, W. D.; Mátyus, E.; Császár, A. G. *Nature* **2008**, *453*, 906–909.
(23) Gerbig, D.; Reisenauer, H. P.; Wu, C.-H.; Ley, D.; Allen, W. D.; Schreiner, P. R. *J. Am. Chem. Soc.* **2010**, *132*, 7273–7275.
(24) Schreiner, P. R.; Reisenauer, H. P.; Ley, D.; Gerbig, D.; Wu, C.-H.; Allen, W. D. *Science* **2011**, *332*, 1300–1303.
(25) Schreiner, P. R.; Reisenauer, H. P. *Angew. Chem., Int. Ed.* **2008**, *47*, 7071–7074.
(26) Larionov, O. V.; de Meijere, A. *Adv. Synth. Catal.* **2006**, *348*, 1071–1078.
(27) Hochstrasser, R.; Wirz, J. *Angew. Chem.* **1989**, *101*, 183–185.
(28) Günther, H. *Tetrahedron Lett.* **1970**, *11*, 5173–5176.
(29) Wiberg, K. B. *Angew. Chem., Int. Ed.* **1986**, *25*, 312–322.
(30) Razavy, M. *Quantum Theory of Tunneling*; World Scientific: Singapore, 2003.
(31) Zhao, Y.; Truhlar, D. G. *Acc. Chem. Res.* **2008**, *41*, 157–167.
(32) Zhao, Y.; Truhlar, D. G. *Theo. Chem. Acc.* **2008**, *120*, 215–241.
(33) Lee, C.; Yang, W.; Parr, R. G. *Phys. Rev. B* **1988**, *37*, 785–789.
(34) Becke, A. D. *J. Chem. Phys.* **1993**, *98*, 5648–5652.
(35) Stephens, P. J.; Devlin, F. J.; Chabalowski, C. F.; Frisch, M. J. *J. Phys. Chem.* **1994**, *98*, 11623–11627.
(36) Čížek, J. *J. Chem. Phys.* **1966**, *45*, 4256–4266.
(37) Raghavachari, K.; Trucks, G. W.; Pople, J. A.; Head-Gordon, M. *Chem. Phys. Lett.* **1989**, *157*, 479–483.
(38) Bartlett, R. J.; Watts, J. D.; Kucharski, S. A.; Noga, J. *Chem. Phys. Lett.* **1990**, *165*, 513–522.
(39) Stanton, J. F. *Chem. Phys. Lett.* **1997**, *281*, 130–134.
(40) Wennmohs, F.; Neese, F. *Chem. Phys.* **2008**, *343*, 217–230.
(41) Neese, F.; Hansen, A.; Wennmohs, F.; Grimme, S. *Acc. Chem. Res.* **2009**, *42*, 641–648.
(42) Dunning, J. T. H. *J. Chem. Phys.* **1989**, *90*, 1007–1023.
(43) CFOUR, Coupled-Cluster Techniques for Computational Chemistry; quantum chemical program package, http://www.cfour.de (see Supporting Information for full reference).
(44) Fukui, K. *J. Phys. Chem.* **1970**, *74*, 4161–4163.
(45) Hratchian, H. P.; Schlegel, H. B. *J. Chem. Phys.* **2004**, *120*, 9918–9924.
(46) Gaussian09, Revision B.02; Gaussian, Inc., Wallingford CT, 2009 (see Supporting Information for full reference).
(47) Mathematica, Version 7.0.1; Wolfram Research Inc., Champaign IL, 2008.